Available online at www.sciencedirect.com

SciVerse ScienceDirect

Ceramics International 38 (2012) 3729–3733

CERAMICS INTERNATIONAL

www.elsevier.com/locate/ceramint

Thermal behavior of the nonstoichiometric lithium niobate powders synthesized via a combustion method

Chia-Liang Kuo [a], Guo-Ju Chen [b], Yee-Shin Chang [c], Jian-Xun Fu [a], Yen-Hwei Chang [a], Weng-Sing Hwang [a,*]

[a] Department of Materials Science and Engineering, National Cheng Kung University, 1 Ta-Hsueh Road, Tainan 70101, Taiwan
[b] Department of Materials Science and Engineering, I-Shou University, Kaohsiung, 1, Syuecheng Rd., Sec. 1 Dashu District, Kaohsiung City 84001, Taiwan
[c] Department of Electronic Engineering, National Formosa University, 64 Wenhua Road, Huwei, Yunlin 632, Taiwan

Received 14 November 2011; received in revised form 6 January 2012; accepted 7 January 2012
Available online 15 January 2012

Abstract

Lithium niobate ($Li_xNb_{1-x}O_{3+\delta}$) powders with various compositions are prepared via combustion synthesis. The thermal properties, crystal structure, and surface morphology of the as-prepared lithium niobate powders are characterized by thermogravimetric and differential thermal analyses (TG/DTA), powder X-ray diffraction (XRD), and scanning electron microscopy (SEM). When the calcination temperature reached 900 °C, the secondary phases Li_3NbO_4 and $LiNb_3O_8$ were observed. The lithium concentration before 900 °C was 40–43%. The lattice parameters increased slightly with decreasing concentration of lithium ions. When the calcination temperature was higher than 900 °C, the major $Li_{0.91}NbO_3$ phase and the minor $LiNbO_3$ phase coexisted in the nonstoichiometric lithium niobate with 43% lithium content.

Keywords: Lithium niobate; Nonstoichiometric; Combustion method; Glycine

1. Introduction

Single crystals of lithium niobate ($LiNbO_3$, LN) and related materials grown via the Czochralski technique are widely used as piezoelectrical, electrooptical, pyroelectrical, and photorefractive materials due to their particular defect structures and outstanding physical properties. A congruent composition has an excess of niobium with respect to a stoichiometric composition. This deviation from stoichiometry is mainly related to the concentration of nonstoichiometric defects.

The bonding energy of Nb–O is stronger than that of Li–O, meaning that the Nb can easily occupy Li sites, and causing light-induced scattering due to the Li vacancies and intrinsic defects, such as anti-site Nb defects [1,2]. With an increasing Li to Nb ratio, the number of intrinsic defects decreases, improving the optical properties. It is well known that these intrinsic defects (anti-site Nb defects or Nb ions occupying Li ion sites and lithium vacancies) are detrimental to the optical properties, and that a decrease in the intrinsic defect concentration can improve the photorefractive properties [3–6].

Most studies of LN and related materials focus on the single-crystal form, with few considering the powder form. There are several methods for synthesizing LN powders, including the solid state reaction, molten nitrate [7], sol–gel [8,9], hydrothermal [10], and combustion methods [11]. Drawbacks of wet chemical synthesis methods are following: difficulty in controlling of chemical compositions and lost of metal ions during washing and precipitation processes. In contrast, the combustion method can obtain uniform, homogeneous, stoichiometric, and nanoscale lithium niobate powders with a diameter of 29–38 nm [11].

Nanoscale lithium niobate powders with various ratios of lithium to niobate can be obtained with the desired composition and structure by using the combustion method at 600 °C for 1 h. The thermal analysis results, crystal structure, and microstructure observation of lithium niobate powders produced via the combustion method are reported in detail in this work.

* Corresponding author. Tel.: +886 6 2757575x62928; fax: +886 6 2344393.
E-mail address: wshwang@mail.ncku.edu.tw (W.-S. Hwang).

0272-8842/$36.00
doi:10.1016/j.ceramint.2012.01.017

2. Experimental procedure

2.1. Sample preparation

$Li_xNb_{1-x}O_{3+\delta}$ ($x = 0.33$, 0.36, . . ., and 0.486) powders were prepared using lithium nitrate ($LiNO_3$) with a purity of 99.4%, ammonium niobate oxalate hydrate ($C_4H_4NNbO_9$) with a purity of 99.99%, and glycine ($C_2H_5NO_2$) with a purity of 99.7% (all supplied by Aldrich Chemical Company, Inc.). 0.5 M stoichiometric aqueous nitrate solutions were prepared from various ratios of reagent-grade $LiNO_3$ to $C_4H_4NNbO_9$, with a glycine to metal nitrate ratio of 3:1. The details of the process can be found in our previous work [11]. The sample with 43% of its lithium niobate metal ions being lithium (i.e., [Li]/([Li] + [Nb]) = 43%) was labeled 43Li-LN. The calcination was conducted at various temperatures for 1 h to observe the structural evolution of the materials.

2.2. Sample characterization

The thermal behaviors of powders were analyzed by thermogravimetry differential thermal analyses (TG/DTA, SETARAM Setsys Evolution Version 16 instrument, France), which were conducted on a 20-mg raw gel at a heating rate of 10 °C/min in air with an empty platinum holder used as the reference. The calcination temperature was determined from the DTA results. The crystal structure was characterized using an X-ray diffractometer (XRD, Model Rad IIA, Rigku Co., Tokyo, Japan) with CuK_α radiation and a Ni filter, operated at 30 kV, and 20 mA with a scanning rate of 0.25°/min.

The surface morphology of the calcined lithium niobate powders was observed with a scanning electron microscope (SEM, Model S-4200, Hitachi Ltd., Tokyo, Japan).

3. Results and discussion

3.1. Thermal analysis of $LiNbO_3$ precursor powders

Fig. 1 shows the DTA–TGA results of the precursor of 48.6Li-LN with a glycine to nitrate ratio of 3:1. The turning points of the TGA curve indicate the temperatures at which the different organic components burn out. After combustion, the nitrate and glycine containing precursor burns into the gases of nitrogen and carbon dioxide, and water. The precursor with a glycine to nitrate ratio of 3:1 is fuel-rich. The DTA curve reveals strong exothermic peaks in the range of 400–600 °C, which result from the violent combustion of glycine. The gases release some heat and reduce the residual energy, preventing grain growth. The reaction is completed above 600 °C, when crystallized lithium niobate oxide powders are produced. The calcination parameters, based on the thermal analysis, are set at 600 °C and 1 h to completely remove the retained carbon from the lithium niobate oxide particles.

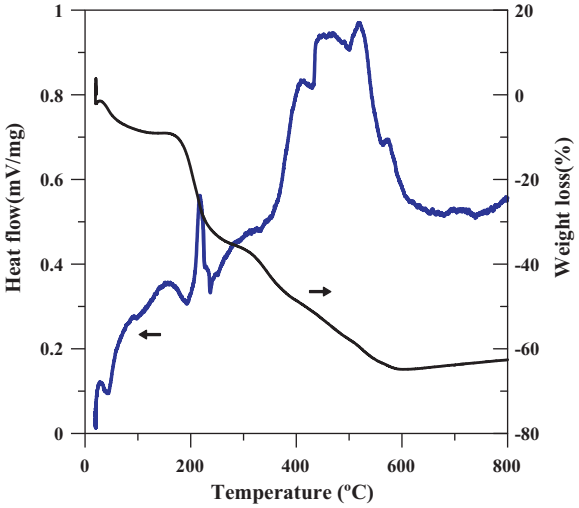

Fig. 1. DTA/TG curves of lithium niobate precursor powders synthesized with a glycine to nitrate ratio of 3:1 and heating rate of 10 °C/min.

3.2. Structure characterization of lithium niobate oxide powders

Fig. 2 shows the X-ray diffraction (XRD) patterns of the as-prepared lithium niobate oxide powders synthesized with various amounts of lithium. After calcination at 600 °C, the precursors transform into metal oxide, and no organic components are observed. When the lithium content is in the range of 0.4–0.486, all the samples show a pure phase of lithium niobate, with no secondary phases. An impurity phase can be

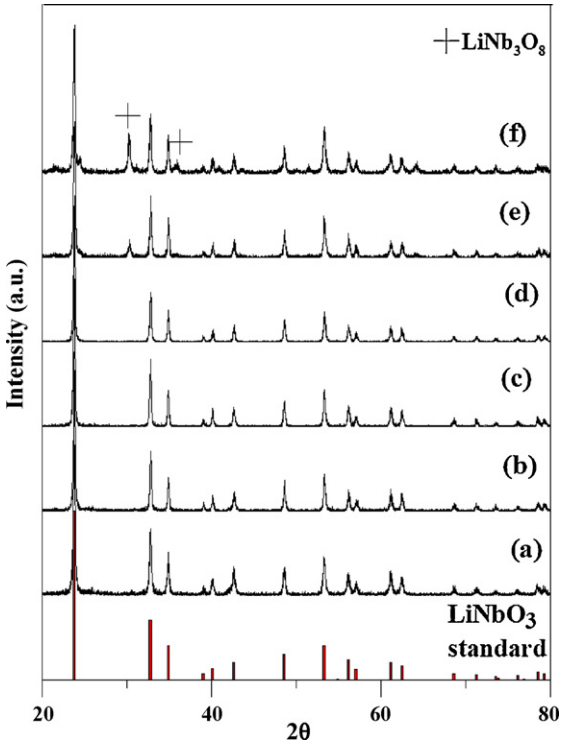

Fig. 2. XRD patterns of lithium niobate precursor powders synthesized at various levels of lithium content calcined at 600 °C for 1 h. (a) 48.6%, (b) 46%, (c) 43%, (d) 40%, (e) 36%, and (f) 33%.

seen at 30° and 62° in Fig. 2(e), which indicates that the lower limit of the lithium concentration for pure lithium niobate is 0.4. When the ratio of lithium to niobium is over 1.5, a niobium-rich secondary phase ($LiNb_3O_8$) appears. Iyi et al. presented the Li-site vacancy model of cation substitution to explain the defects in nonstoichiometric lithium niobate [1]. In the Li-site vacancy model, niobium ions occupy the lithium vacancy sites, and the occupying niobium ions change their electronic state from Nb^{5+} to Nb^{3+} to balance the electric neutrality, and then leave the vacancies. The concentration of lithium ions is inversely proportional to the concentration of the vacancies and the substituted niobium ions. The lattice parameters of nonstoichiometric lithium niobate slightly decrease with the increasing Li content, and the results are shown in Table 1.

After calcination at over 900 °C, two peaks are observed at 26° and 33.6°, which correspond to the lithium-rich secondary phase Li_3NbO_4. With increasing calcination temperature, the solubility of lithium ions in lithium niobate decreases. The Li_3NbO_4 phase decomposes from the relatively high concentration of lithium when the lithium content is over 0.46. The lithium content required in lithium niobate nanopowders to stabilize the pure lithium niobate phase is in the range of 0.40–0.43. The nano effect lowers the equilibrium temperature. The approximate phase diagram for lithium niobate is obtained by observing the single crystals seeded by $LiNbO_3$, which remain stable for a long time. The dispersion of ions tends to follow the $LiNbO_3$ structure. The ions of as-prepared lithium niobate nano-powders, which contain a great amount of free surface energy, organize themselves. Because the solubility limit increases with decreasing temperature, the niobium rich lithium niobate exhibits a large range of solid-solution lithium ratios in lithium niobate at low temperatures (Fig. 3).

The XRD patterns of the 43Li-LN sample calcined at various temperatures for 1 h are shown in Fig. 4. The calcined 43Li-LN sample exhibits the pure phase of lithium niobate, with no secondary phases. When the calcination temperature was below 1000 °C, the ratio of the diffraction peaks of the 43Li-LN sample fitted the standard value (JCPD card number 85-2456). As the calcination temperature increased, the crystallization of the (1 0 4) and (2 0 8) planes increased abnormally, and the elements tended to arrange themselves in the loosening plane. When the calcination temperature approached the melting point (1150 °C), several crystal planes vanished, and the structure became a single crystal. The structure of 43Li-LN at 1050 °C belongs to the metastable

Table 1
Lattice parameters and unit-cell volume for various compositions (x) in the system $Li_xNb_{1-x}O_{3+\delta}$ calcined at 600 °C for 1 h.

Lithium content	Lattice parameters		
	a (Å)	c (Å)	Unit-cell volume (Å^3)
40%	5.1586	13.8939	320.1976
43%	5.153	13.8995	319.6354
46%	5.1525	13.8789	319.0944
48.6%	5.1484	13.8585	318.1233

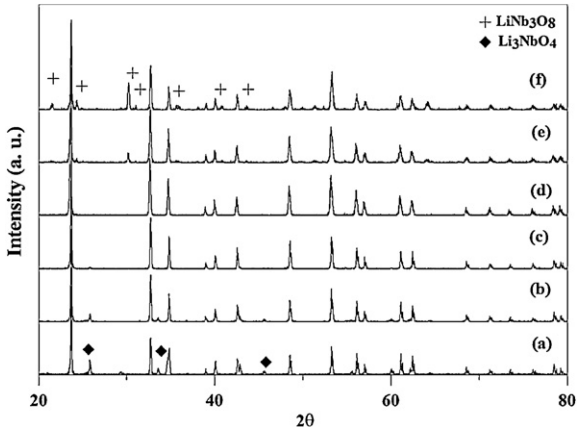

Fig. 3. XRD patterns of lithium niobate precursor powders with various levels of lithium content calcined at 900 °C for 1 h. (a) 48.6%, (b) 46%, (c) 43%, (d) 40%, (e) 36%, and (f) 33%.

phase, the (1 0 4) and (2 0 8) planes have abnormal growth, and the intensity of the two planes reduces at higher temperatures.

The XRD patterns of the (0 2 4), (1 1 6), and (2 0 8) reflections for 43Li-LN powders calcined at various temperatures are shown in Fig. 5. Single and sharp peaks are observed for 43Li-LN powder calcined at 800 °C. The (0 2 4) and (1 1 6) reflections split clearly and shift to the left with increasing calcination temperature. The (2 0 8) reflection has abnormal growth and splits into two peaks completely at 1050 °C. This separation of reflections is due to the phase segregation of the major $Li_{0.91}NbO_3$ phase and the minor $LiNbO_3$ phase. With increasing calcination temperature, the structure of $Li_{0.43}Nb_{0.57}O_{3+\delta}$ with a large amount of vacancy defects tends to divide

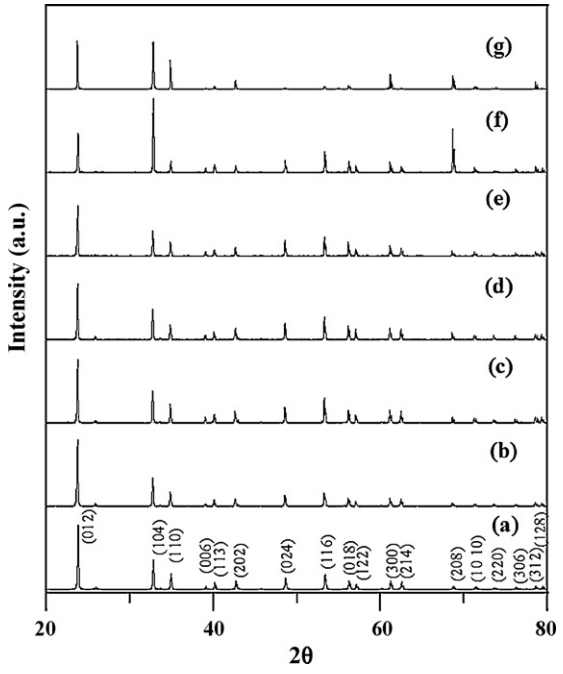

Fig. 4. XRD patterns of 43Li-LN calcined at various temperatures for 1 h. (a) 800 °C, (b) 850 °C, (c) 900 °C, (d) 950 °C, (e) 1000 °C, (f) 1050 °C, and (g) 1100 °C.

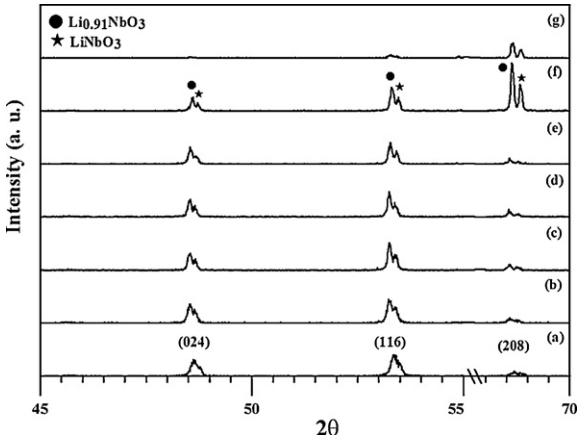

Fig. 5. XRD patterns of the (0 2 4), (1 1 6), and (2 0 8) reflections for 43Li-LN for calcination temperatures of (a) 800 °C, (b) 850 °C, (c) 900 °C, (d) 950 °C, (e) 1000 °C, (f) 1050 °C, and (g) 1100 °C.

into stoichiometric lithium niobate ($LiNbO_3$) and non-stoichiometric lithium niobate $Li_{0.91}NbO_3$, reducing the number of defects in the $Li_{0.43}Nb_{0.57}O_{3+\delta}$ crystals.

3.3. Surface morphology of lithium niobate oxide powders

The surface morphology of lithium niobate particles calcined at various temperatures is observed using scanning electron microscopy. Fig. 6 shows that after calcining at 900 °C, the particle size is about 100 nm, twice that obtained after calcining at 600 °C [11]. When the calcination temperature rises to 950 °C, the particle size increases threefold. The original scale bar is too narrow to fit the particles calcined at 1050 °C, and thus; it is changed to 10 μm for samples calcined at higher temperatures. As the calcination temperature approaches the melting temperature, the particle growth rate increased rapidly. The highest calcination temperature is

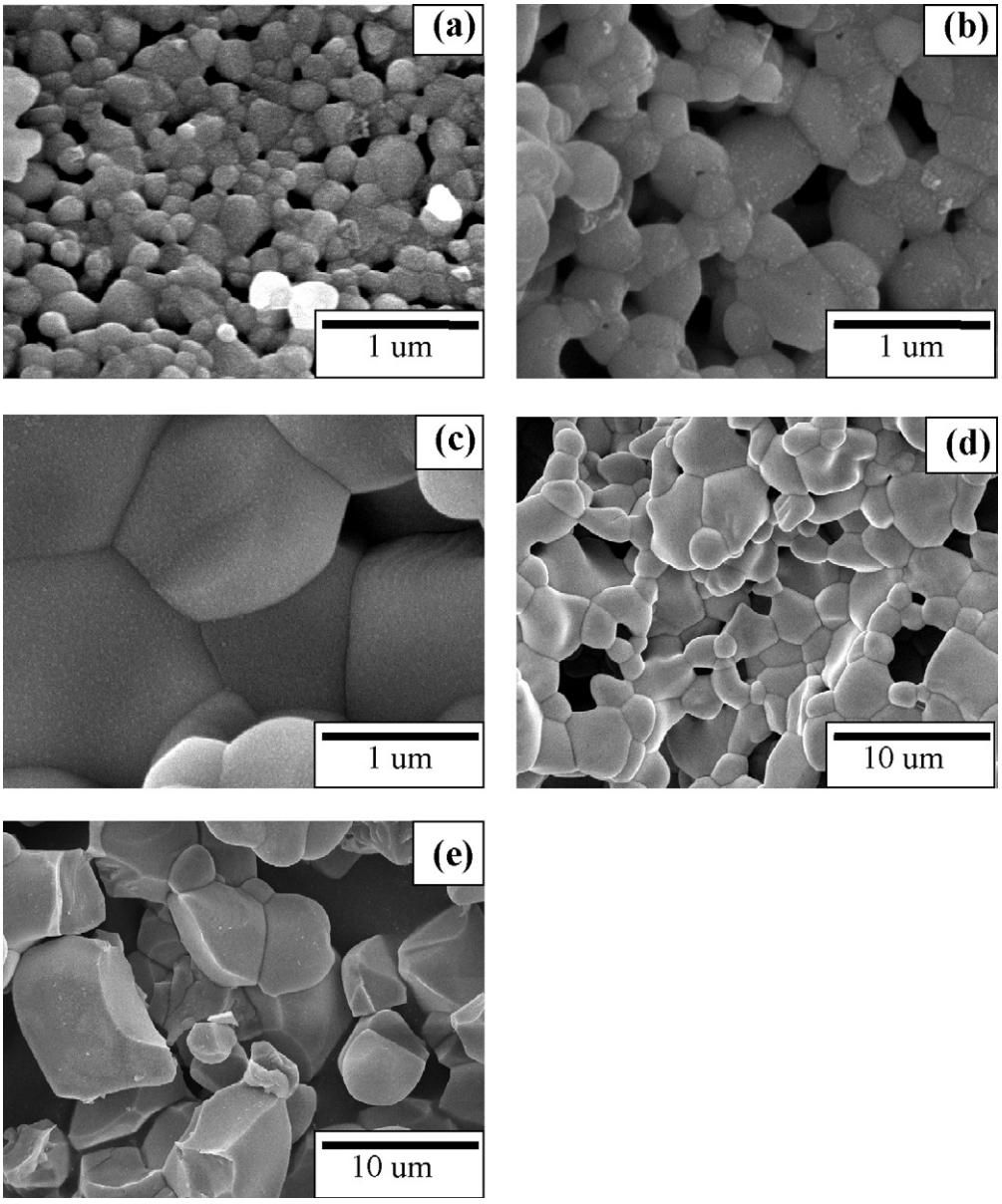

Fig. 6. SEM images of 43Li-LN powders calcined at various temperatures for 1 h. (a) 900 °C, (b) 950 °C, (c) 1000 °C, (d) 1050 °C, and (e) 1100 °C.

1100 °C because the LN melts at temperatures above this, and the particles thus obtained are in the range of 5–10 μm. The grain growth of the lithium niobate particles is proportional to the calcination temperature for temperatures higher than 900 °C.

4. Conclusion

The thermal behavior of lithium niobate ($Li_xNb_{1-x}O_{3+\delta}$) powders synthesized via a combustion method is reported in this work, and the following results are obtained:

1. The suitable concentration of lithium ions in lithium niobate powders synthesized via the combustion method is in the range of 40–43% if the single phase of $LiNbO_3$ is obtained at high temperature.
2. With a decrease in the lithium concentration, the lattice parameters and unit volume of lithium niobate increase.
3. The major $Li_{0.91}NbO_3$ phase and the minor $LiNbO_3$ phase are formed in 43Li-LN when the calcination temperature is higher than 950 °C, and a reduction in defects is observed by nonstoichiometry.
4. The nanoscale lithium niobate powders have significant grain growth when the calcination temperature is higher than 900 °C.

Acknowledgements

The authors would like to thank the National Science Council of Taiwan for financially supporting this research (NSC 100-2221-E-006-091-MY3, NSC 100-2811-E-006-004-), and the Towards the Top-Tier University and Elite Research Center Development Plan promoted by the Ministry of Education of Taiwan (D100-23003).

References

[1] N. Iyi, K. Kitamura, F. Izumi, J.K. Yamamoto, T. Hayashi, H. Asano, S. Kimura, Comparative study of defect structures in lithium niobate with different compositions, J. Solid State Chem. 101 (1992) 340–352.
[2] G. Malovichko, V. Grachev, O. Schirmer, Interrelation of intrinsic and extrinsic defects congruent, stoichiometric, and regularly ordered lithium niobate, Appl. Phys. B 68 (1999) 785–793.
[3] X. Yue, A. Adibi, T. Hudson, K. Buse, D. Psaltis, Lifetime of small polarons in iron-doped lithium-niobate crystals, J. Appl. Phys. 87 (2000) 1034–1041.
[4] Y. Liu, K. Kitamura, G. Ravi, S. Takekawa, M. Nakamura, Growth and two-color holographic storage properties of Mn-doped lithium niobate crystals with varying Li/Nb ratio, J. Appl. Phys. 96 (2004) 5996–6001.
[5] R. Bhatt, S. Kar, K.S. Bartwal, The effect of Cr doping on optical and photoluminescence properties of $LiNbO_3$ crystals, Solid State Commun. 127 (2003) 457–462.
[6] Y. Furukawa, K. Kitamura, S. Takekawa, K. Niwa, Y. Yajima, N. Iyi, I. Mnushkina, P. Guggenheim, J.M. Martin, The correlation of MgO-doped near-stoichiometric $LiNbO_3$ composition to the defect structure, J. Cryst. Growth 211 (2000) 230–236.
[7] P. Afanasiev, Synthesis of microcrystalline $LiNbO_3$ in molten nitrate, Mater. Lett. 34 (1998) 253–256.
[8] B. Knabe, D.S. Schutze, T. Jungk, M. Svete, W. Assenmacher, W. Mader, K. Buse, Synthesis and characterization of Fe-doped $LiNbO_3$ nanocrystals from a triple-alkoxide method, Phys. Status Solidi A 208 (2011) 857–862.
[9] Z. Cheng, K. Ozawa, A. Miyazaki, H. Kimura, Formation of lithium niobate from peroxide aqueous solution, J. Am. Ceram. Soc. 88 (2005) 1023–1025.
[10] M. Liu, D. Xue, K. Li, Soft-chemistry synthesis of $LiNbO_3$ crystallites, J. Alloys Compd. 449 (2008) 28–31.
[11] C.L. Kuo, Y.S. Chang, Y.H. Chang, W.S. Hwang, Synthesis of nanocrystalline lithium niobate powders via a fast chemical route, Ceram. Int. 37 (2011) 951–955.